

Effects of Palladium Doping on the Structure and Electrochemical Properties of LiFePO₄/C Prepared using the Sol-gel Method

M. Talebi-Esfandarani and O. Savadogo*

Laboratory of New Materials for Electrochemistry and Energy, École Polytechnique de Montréal,
C.P. 6079, Succ. Centre Ville, Montréal, QC, Canada, H3C 3A7

Received: November 21, 2013, Accepted: January 24, 2014, Available online: May 09, 2014

Abstract: LiFePO₄/C, LiFe_{0.98}Pd_{0.02}PO₄/C, and LiFe_{0.96}Pd_{0.04}PO₄/C composite cathode materials were synthesized using the sol-gel method. The effect of palladium on the structure and electrochemical properties of LiFePO₄/C have been investigated by X-ray diffraction (XRD), X-ray photoelectron spectroscopy (XPS), scanning electron microscopy (SEM), surface area measurement (BET), charge/discharge testing, and cyclic voltammetry (CV). The results indicate that palladium doping facilitates the formation of impurities, like Li₃PO₄. Also, the lattice parameters of the LiFePO₄ structure decrease in size as the palladium content increases. In addition, the particles become larger and agglomerated by palladium incorporation. The electrochemical results show that palladium doping decreases the electrochemical performance of LiFePO₄/C, owing to shrinking lattice parameters and the difficulty of achieving the diffusion of lithium ions into the structure during the intercalation/de-intercalation process. These results suggest that palladium doping by sol-gel method changes significantly the LiFePO₄ structure which may impact its performances as cathode for the lithium ion battery applications.

Keywords: LiFePO₄/C, sol-gel method, palladium doping, lithium ion diffusion.

1. INTRODUCTION

Since 1997, LiFePO₄ has been a promising candidate as a cathode material in lithium ion battery applications, because of its excellent thermal stability, low cost, non toxicity, and abundance in nature [1-3]. However, pristine LiFePO₄ suffers from poor ion diffusion (10^{-14} cm²s⁻¹) and low electrical conductivity (10^{-9} Scm⁻¹), which result in low current densities, limiting its application in large electronics [4, 5]. Various approaches have been proposed to solve these problems, such as decreasing particle size reduction, carbon coating, and metal doping [6-12]. Experimental results and theoretical studies show that metal doping is more complex than carbon coating and particle size reduction. Moreover, the doping mechanism is not yet clearly understood. It has been demonstrated that small particles facilitate the passage of Li ions through the LiFePO₄ structure [10], that carbon coating improves the electronic properties on the surface of the LiFePO₄ particles [13], and that a doping agent can increase the intrinsic electrical conductivity of bulk LiFePO₄ particles [14-16]. A doping agent can also make a longer Li-O bond with a lower energy barrier

in the LiFePO₄ structure, so that Li ion movement becomes easier, enhancing the ionic conductivity [17-19]. However, doping bulk LiFePO₄ material without a carbon coating is not enough to improve its electrochemical performance. As a result, researchers usually combine the doping and carbon coating elements in order to achieve this improvement.

To select an appropriate doping approach, many factors must be considered, including the site of the doping, the physicochemical properties of the dopant, and the amount of dopant required. Theoretical studies have shown that LiFePO₄ has a one-dimensional Li ion diffusion pathway [21-23], and that a non mobile dopant at the Li site probably blocks the diffusion of Li ions [24, 25]. Also, a very large amount of dopant may block the diffusion channels for Li ions throughout the LiFePO₄ structure, and also collapse or destroy that structure [11, 25, 26]. However, it has been reported that various dopant elements enhance the electrochemical performance of LiFePO₄, including Sn [14], Mg [15], La [26], Na [27], Cu [28], V [29], Ti [30], Co [31], Ru [32], Mo [33], F [34], Cl [35], Zn [36], Cr [37], etc.

So far, to our knowledge, the effect of palladium (Pd) on LiFePO₄ has not been reported. In this paper, we introduce a meth-

*To whom correspondence should be addressed: Email: osavadogo@polymtl.ca
Phone: +1 514 3404725

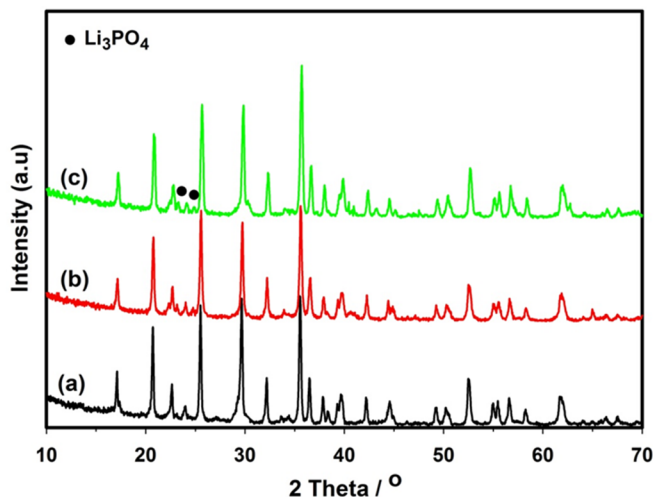


Figure 1. XRD patterns of: (a) LiFePO_4 , (b) $\text{LiFe}_{0.98}\text{Pd}_{0.02}\text{PO}_4$, and (c) $\text{LiFe}_{0.96}\text{Pd}_{0.04}\text{PO}_4$ samples.

od for synthesizing Pd-doped LiFePO_4 material using the sol-gel method, and investigate the effect of Pd doping on the physical and electrochemical properties of the prepared materials.

2. EXPERIMENTAL

2.1. Synthesis of materials

LiFePO_4 , $\text{LiFe}_{0.98}\text{Pd}_{0.02}\text{PO}_4$, and $\text{LiFe}_{0.96}\text{Pd}_{0.04}\text{PO}_4$ samples were synthesized using the sol-gel method and a stoichiometric amount of $\text{Li}(\text{CH}_3\text{COO})$ (lithium acetate, Alfa Aesar), $\text{Fe}(\text{NO}_3)_3 \cdot 9\text{H}_2\text{O}$ (iron nitrate, Sigma Aldrich), $\text{Pd}(\text{NO}_3)_2 \cdot 2\text{H}_2\text{O}$ (palladium nitrate, Sigma Aldrich), and H_3PO_4 (phosphoric acid, Anachemia). First, phosphoric acid was diluted in the distilled water, and then iron nitrate, palladium nitrate, and lithium acetate were added to the solution, which was mixed until the constituents were completely dissolved. The solution was combined with glycolic acid and the pH was adjusted to fall into the 8.5 to 9.5 range using ammonium hydroxide. The solution was heated at 90°C while stirring until a gel formed. After drying at 120°C in a vacuum oven, the sample was annealed at 500°C for 10 h to obtain LiFePO_4 . Finally, the presynthesized LiFePO_4 was mixed with sucrose as a carbon source in a 70:30 weight ratio, followed by annealing at 700°C for 5 h to prepare a LiFePO_4/C composite. The procedure was performed under a nitrogen atmosphere.

2.2. Materials characterization

The phase purity and crystalline structure of the samples were investigated using an X-ray diffractometer (Philips X'pert) with $\text{CuK}\alpha$ radiation ($\lambda=1.54056 \text{ \AA}$). The oxidation states of the Fe and Pd ions were analyzed by X-ray photoelectron spectroscopy (VG ESCALAB 3 MKII) with an $\text{Al K}\alpha$ radiation source ($h\nu=1486.6 \text{ eV}$). The pressure in the analyzer chamber was around 8^{-9} Torr with a power of 216 W and a $2 \times 3 \text{ mm}$ analysis region. The data were calibrated with respect to a C1s peak at a value of 285.0 eV. Their morphology and particle size distributions were observed by scanning electron microscopy (JSM-7600TFE), and their specific surface area was determined using a BET measurement machine

(Autosorb-1, Quantachrome instruments). The carbon content of the samples was measured by carbon analyzer (LECO Co., CS 400).

2.3. Electrochemical characterization

The composite cathodes for electrochemical measurement were prepared by mixing the LiFePO_4/C powders, carbon black (Super C65-Timcal), and polyvinylidene fluoride (PVDF) in a weight ratio of 80:10:10 in an N-methyl-2-pyrrolidone solvent for 3-6 h. Subsequently, the slurry was coated onto aluminum foil using the doctor blade technique and dried in a vacuum oven overnight. The cells (2032) were assembled in an argon-filled glove box with lithium metal as the anode, a Celgard 2400 as the separator, and 1 molL^{-1} LiPF_6 in ethylene carbonate-dimethyl carbonate as the electrolyte. The charge/discharge test and cycling stability test were performed between 2.5 and 4.2V (vs. Li/Li^+) with a Solartron battery test analyzer. Cyclic voltammetry (CV) was carried out using PAR273A in the potential range of 2.5-4.2V (vs. Li/Li^+) with scan rates of 0.1 mV/s. All the electrochemical measurements were carried out at room temperature.

3. RESULTS AND DISCUSSION

Fig. 1 shows the XRD patterns for the LiFePO_4 , $\text{LiFe}_{0.98}\text{Pd}_{0.02}\text{PO}_4$, and $\text{LiFe}_{0.96}\text{Pd}_{0.04}\text{PO}_4$ samples. For all the samples, the main diffraction peaks indexed a standard olivine LiFePO_4 phase with an orthorhombic structure, a space group of P_{mnb} (JCPDS 40-1499). The Pd-doped samples contain the Li_3PO_4 impurity phase. As the palladium content increases, the intensities of the Li_3PO_4 diffraction peaks are enhanced, indicating that palladium incorporation facilitates the formation of the Li_3PO_4 impurity. However, the Li_3PO_4 phase has usually been reported as an impurity in doped LiFePO_4 samples [27, 38]. At the same time, Li_3PO_4 might act as an inert and inactive mass, decreasing the electrochemical performance of LiFePO_4 material [39, 40].

The lattice parameters of the samples were calculated using Topas software, and are listed in Table 1. These parameters demonstrate that palladium has been successfully doped into the LiFePO_4 phase. They decrease along with their cell volume, with an increasing amount of palladium. Therefore, the shrinkage in the lattice parameters delays Li ion insertion and extraction throughout the structure of the LiFePO_4 , because there is less space available for diffusion [17, 19, 32,41]. This probably blocks channel diffusion, consequently decreasing the electrochemical performance of the cathode materials, especially under the high C rate, which is compatible with Islam's suggestion [23]. These results seem to be inconsistent with the expectation that the lattice parameters increase with an increasing amount of Pd^{2+} replacement of Fe^{2+} ions, since

Table 1. Lattice parameters of pristine and doped LiFePO_4 from XRD data

Sample	a(Å)	b(Å)	c(Å)	V
LiFePO_4	10.32408	6.00286	4.69050	290.689
$\text{LiFe}_{0.98}\text{Pd}_{0.02}\text{PO}_4$	10.31850	6.00157	4.69036	290.461
$\text{LiFe}_{0.96}\text{Pd}_{0.04}\text{PO}_4$	10.31470	5.99609	4.68602	289.820

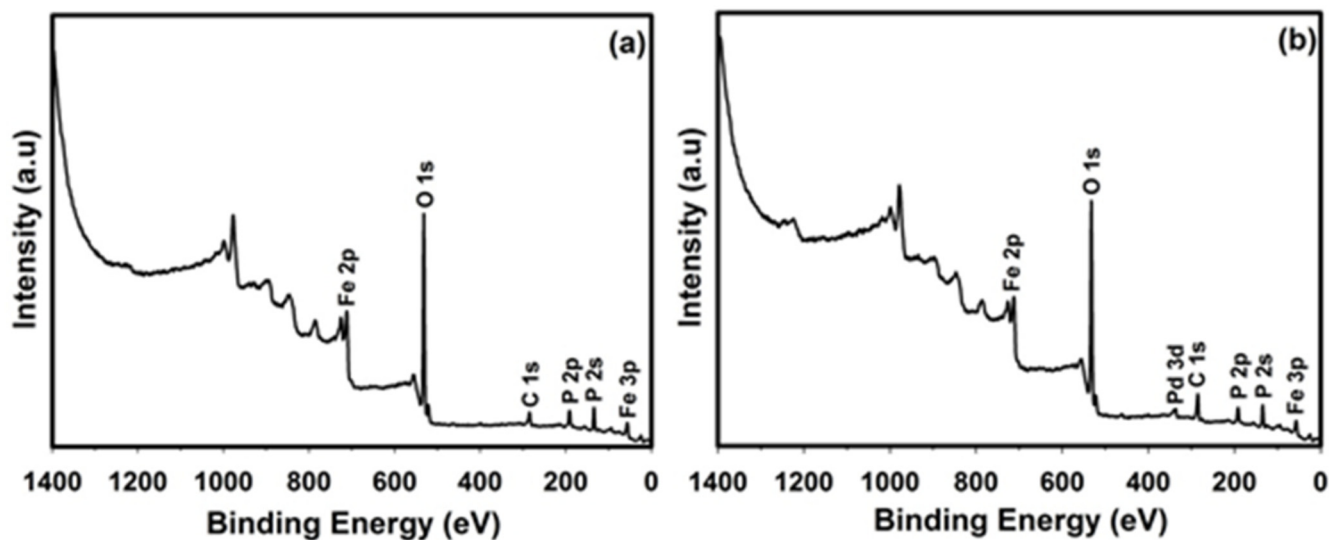


Figure 2. XPS spectra of the samples: (a) LiFePO_4 ; and (b) $\text{LiFe}_{0.96}\text{Pd}_{0.04}\text{PO}_4$.

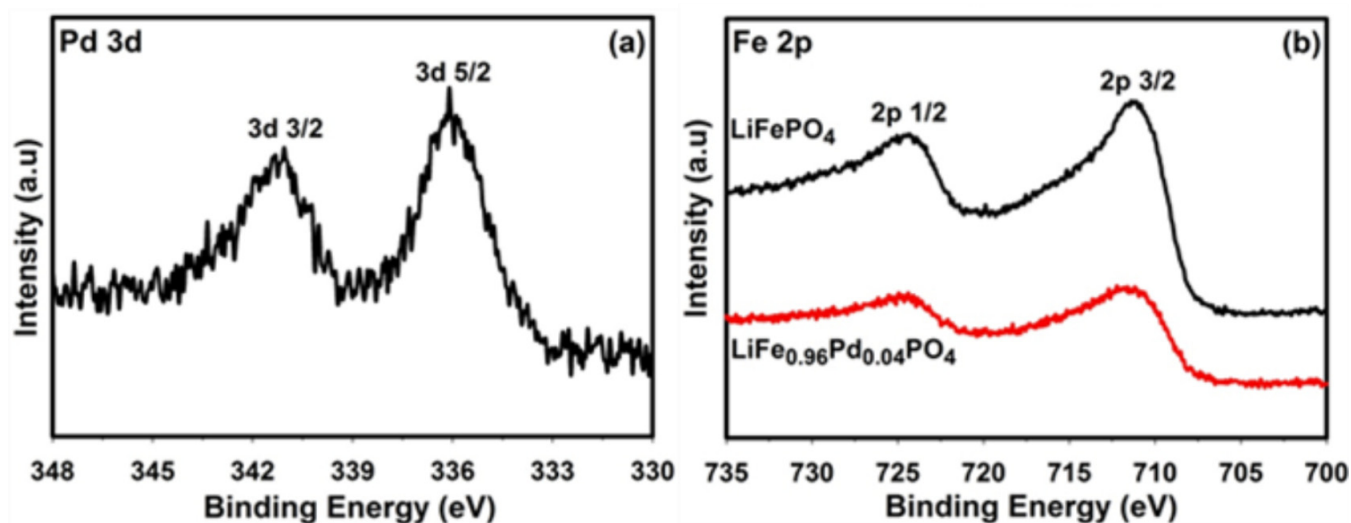


Figure 3. (a) XPS core levels of Pd 3d for the $\text{LiFe}_{0.96}\text{Pd}_{0.04}\text{PO}_4$ sample; (b) XPS core levels of Fe 2p for the LiFePO_4 and $\text{LiFe}_{0.96}\text{Pd}_{0.04}\text{PO}_4$ samples.

the ionic radius of Pd^{2+} (86\AA) is larger than that of Fe^{2+} (78\AA). The same unexpected result has been reported for Ti-doped LiFePO_4 [38].

The oxidation states of Fe and Pd for the LiFePO_4 and $\text{LiFe}_{0.96}\text{Pd}_{0.04}\text{PO}_4$ samples can be determined by XPS analysis. The XPS spectra within a wide range of binding energies for the LiFePO_4 and $\text{LiFe}_{0.96}\text{Pd}_{0.04}\text{PO}_4$ samples are illustrated in Fig. 2. The peaks corresponding to Fe 2p, O 1s, P 2p, and C 1s were observed for both samples, as indicated in Fig. 2. The binding energy for the Li 1s peak overlaps the Fe 3p peak (56 eV), and so it was not feasible to determine its binding energy or approximate its element content. Note that the Pd 3d peak was observed for the doped sample, as shown in Fig. 2(b), confirming the existence of Pd in the sample.

Fig. 3(a) shows the high resolution spectrum for the Pd 3d peak in the doped sample. It contains a doublet with binding energies of 336 eV and 341 eV, corresponding to the Pd 3d_{5/2} and Pd 3d_{3/2} lines respectively, which determines that the oxidation state of Pd in the doped sample is +2 [42]. In order to examine the effect of Pd doping on the oxidation state and binding energy of Fe, the high-resolution spectra of the Fe 2p peak for the two samples were compared, as illustrated in Fig. 3(b). LiFePO_4 samples contain the Fe 2p_{3/2} (710.9 eV) and Fe 2p_{1/2} (724 eV) peaks, indicating that the oxidation state of the Fe is +2, which is compatible with other reports [31, 41]. For the doped sample, no obvious changes were observed in comparison with the LiFePO_4 sample, indicating that the doping of Pd does not significantly change the valence of Fe^{2+} .

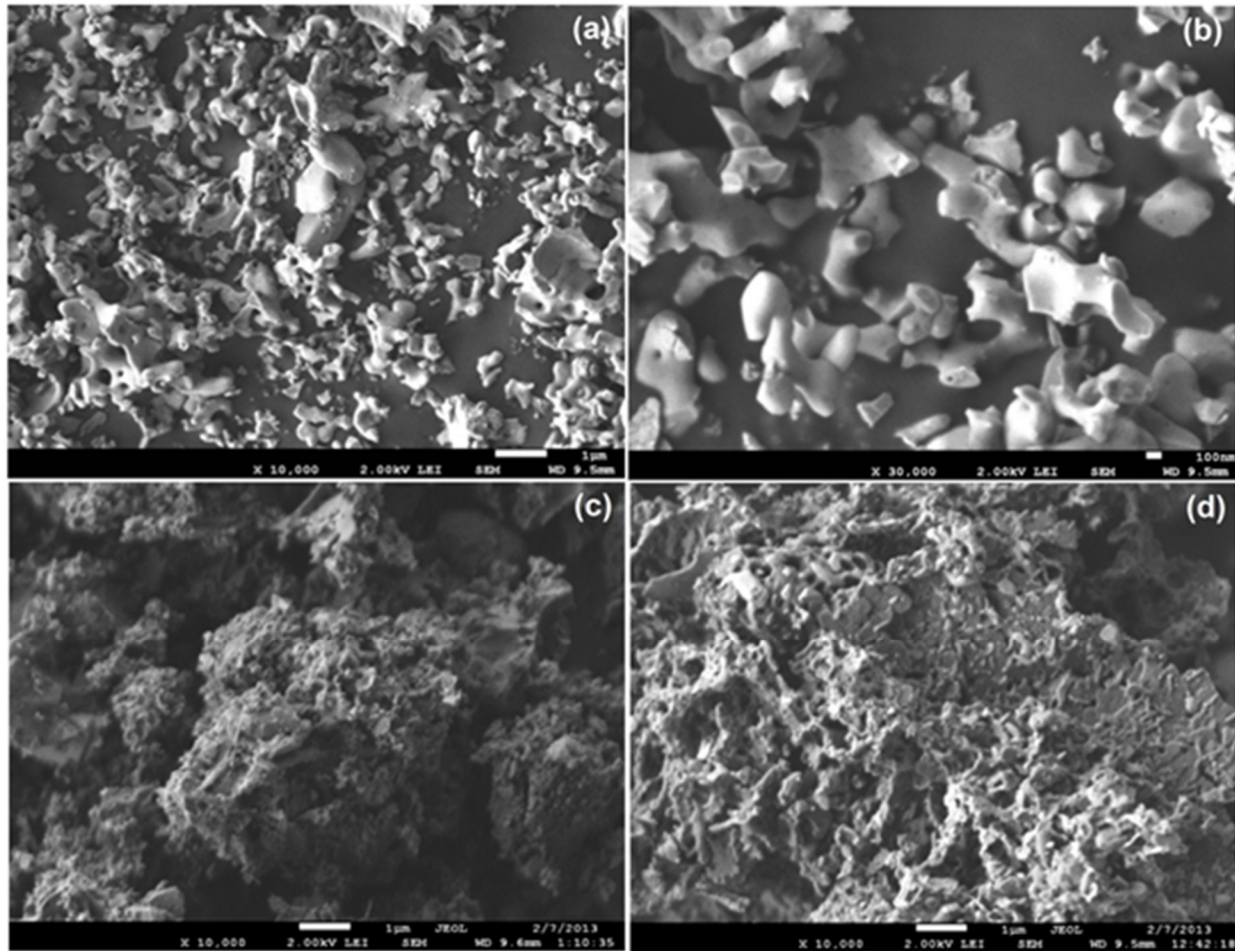


Figure 4. SEM images of (a) LiFePO_4 , (b) High resolution LiFePO_4 , (c) $\text{LiFe}_{0.98}\text{Pd}_{0.02}\text{PO}_4$, and (d) $\text{LiFe}_{0.96}\text{Pd}_{0.04}\text{PO}_4$.

Fig. 4 shows the SEM images of the LiFePO_4 , $\text{LiFe}_{0.98}\text{Pd}_{0.02}\text{PO}_4$, and $\text{LiFe}_{0.96}\text{Pd}_{0.04}\text{PO}_4$ samples. The LiFePO_4 material consists of small homogeneous particles 100-500 nm in size, as shown in Fig. 4(b). However, palladium incorporation changes the morphology of this material completely, and the particles become larger (1-5 μm) and agglomerated. This explains its lower electrochemical capacity, as discussed later. However, agglomeration in the doped samples may be caused by the Li_3PO_4 phase, in which melting may have occurred during the calcination process [31]. Also, the specific surface area of the samples decreases with increasing palladium content, as shown in Table 2. Therefore, the amount of surface area for the reaction reduces with palladium incorporation. It is believed that small, regular particles tend to reduce the length of the path of

Li ions diffusing through the structure, resulting in fast reaction and diffusion kinetics for the intercalation/de-intercalation process, which can enhance the electrochemical performance of LiFePO_4 material.

Fig. 5 shows the charge and discharge curves of the LiFePO_4/C , $\text{LiFe}_{0.98}\text{Pd}_{0.02}\text{PO}_4/\text{C}$, and $\text{LiFe}_{0.96}\text{Pd}_{0.04}\text{PO}_4/\text{C}$ samples at different C-rates between 2.5 and 4.2 V. The LiFePO_4/C sample shows a flat voltage plateau at around 3.4 V, related to a two-phase $\text{Fe}^{3+}/\text{Fe}^{2+}$ redox reaction process between FePO_4 and LiFePO_4 . The LiFePO_4/C sample achieves the specific capacity of 164, 150, 120, and 105 mAh/g at rates of 0.2C, 1C, 5C, and 10C respectively. Palladium substitution decreases the discharge capacity of the samples, and a further decrease in the discharge capacity is observed when the palladium content is increased. This is partly due to the existence of the Li_3PO_4 impurity phase, as palladium incorporation facilitates the formation of the Li_3PO_4 impurity. This impurity can act as an inert and inactive mass during the redox process, reducing electrochemical performance [39, 40]. Another possibility is that the lattice parameters decrease with an increasing palladium content, and parameter shrinkage makes it difficult for Li ions to diffuse into the structure of LiFePO_4 . This is because there is less space available for diffusion, which is blocked as a result. Also, the

Table 2. BET result of the samples

Sample	Specific surface area(m^2/g)
LiFePO_4/C	43.7
$\text{LiFe}_{0.98}\text{Pd}_{0.02}\text{PO}_4/\text{C}$	40.7
$\text{LiFe}_{0.96}\text{Pd}_{0.04}\text{PO}_4/\text{C}$	33.5

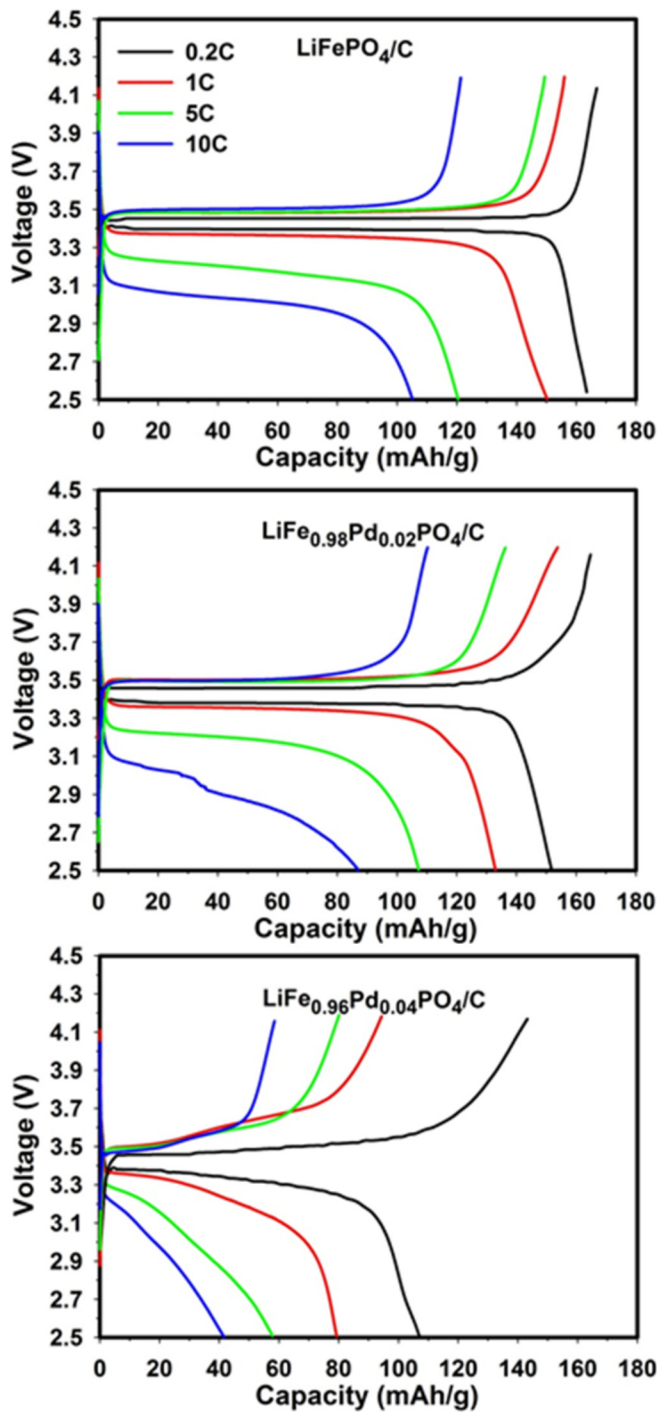


Figure 5. Charge and discharge curves for the LiFePO_4/C , $\text{LiFe}_{0.98}\text{Pd}_{0.02}\text{PO}_4/\text{C}$, and $\text{LiFe}_{0.96}\text{Pd}_{0.04}\text{PO}_4/\text{C}$ samples at various rates.

large size and agglomeration of the particles, as shown in the SEM results, delay Li ion diffusion during the reaction process that the Pd-doped samples undergo. However, in the case of the $\text{LiFe}_{0.96}\text{Pd}_{0.04}\text{PO}_4/\text{C}$ sample, a flat plateau is not observed, clearly confirming higher polarization, owing to the extra Li_3PO_4 impurity

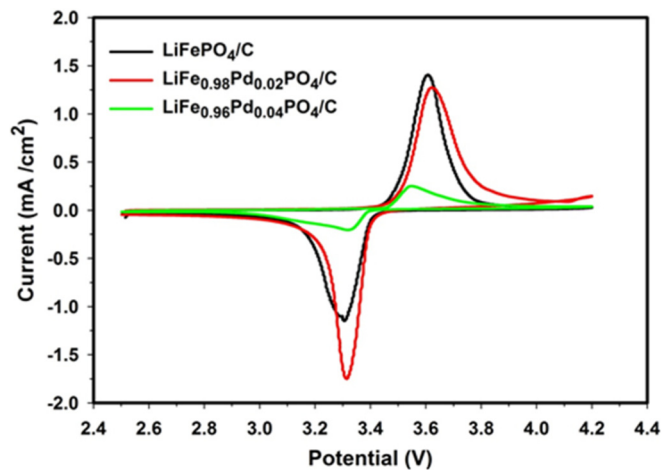


Figure 6. CV curves of the LiFePO_4/C , $\text{LiFe}_{0.98}\text{Pd}_{0.02}\text{PO}_4/\text{C}$, and $\text{LiFe}_{0.96}\text{Pd}_{0.04}\text{PO}_4/\text{C}$ samples.

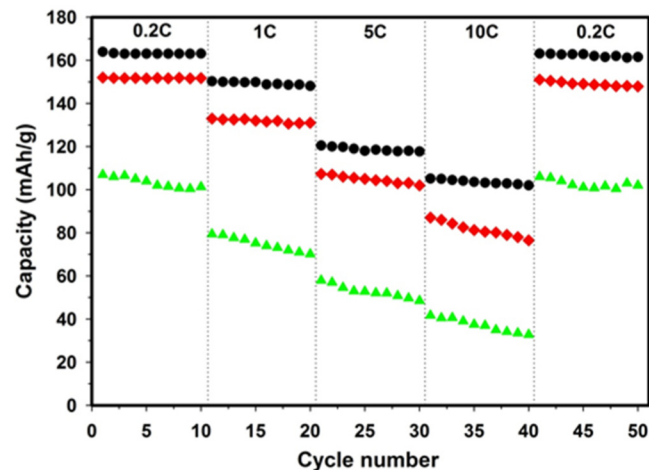


Figure 7. Cycling performance of the LiFePO_4/C (●), $\text{LiFe}_{0.98}\text{Pd}_{0.02}\text{PO}_4/\text{C}$ (◻), and $\text{LiFe}_{0.96}\text{Pd}_{0.04}\text{PO}_4/\text{C}$ (▲) samples at various discharge rates.

phase and the limitation of Li ion diffusion. The $\text{LiFe}_{0.96}\text{Pd}_{0.04}\text{PO}_4/\text{C}$ sample achieves the low specific capacity of 107, 79, 58, and 42 mAh/g at rates of 0.2C, 1C, 5C, and 10C respectively. Murugan et al. also report that cobalt doping does not have a positive effect on the electrochemical properties of LiFePO_4/C [43].

In all three samples, the carbon contents in the final cathode materials were around 6.8 wt%. The effects of palladium doping on the electrochemical properties of LiFePO_4/C materials can be further investigated by cyclic voltammograms. Fig. 6 shows the CV curves of LiFePO_4/C , $\text{LiFe}_{0.98}\text{Pd}_{0.02}\text{PO}_4/\text{C}$, and $\text{LiFe}_{0.96}\text{Pd}_{0.04}\text{PO}_4/\text{C}$ samples between 2.5 and 4.2V at a scan rate of 0.1 mV/s. For all the samples, the oxidation/reduction peaks, attributed to the reaction of the $\text{Fe}^{2+}/\text{Fe}^{3+}$ redox couple, were clearly observed. However, the LiFePO_4/C sample shows more symmetry in its anodic/cathodic peaks, and the peaks are sharper, suggesting better electrochemical

properties. Although the $\text{LiFe}_{0.96}\text{Pd}_{0.04}\text{PO}_4/\text{C}$ sample shows less separation between its anodic/cathodic peaks, the amount of current is very low in comparison with that of other samples. The results indicate that Li ion insertion and extraction can be achieved more easily in the LiFePO_4/C sample.

The discharge cycling tests at various rates for the LiFePO_4/C , $\text{LiFe}_{0.98}\text{Pd}_{0.02}\text{PO}_4/\text{C}$, and $\text{LiFe}_{0.96}\text{Pd}_{0.04}\text{PO}_4/\text{C}$ samples are shown in Fig. 7. Here, the LiFePO_4/C sample can be seen to exhibit good capacity retention at various discharge rates. Moreover, its capacity can be completely recovered when the rate is decreased from 10 C to 0.2 C. However, capacity fading can be observed when the amount of palladium doping is increased, especially for the $\text{LiFe}_{0.96}\text{Pd}_{0.04}\text{PO}_4/\text{C}$ sample in high-rate tests, which indicates poor cycling stability. The poor electrochemical performance and cycling of the Pd-doped samples, especially the $\text{LiFe}_{0.96}\text{Pd}_{0.04}\text{PO}_4/\text{C}$ sample, can be attributed to the formation of the Li_3PO_4 impurity phase, shrinkage of the lattice parameters, agglomeration, and large particle size, which result in the difficulty of diffusing Li ions into the structure during the intercalation/de-intercalation process. However, this examination indicates that doping at the Fe site with Pd^{2+} does not improve the electrochemical properties of the LiFePO_4/C material for lithium ion battery applications.

4. CONCLUSIONS

LiFePO_4 , $\text{LiFe}_{0.98}\text{Pd}_{0.02}\text{PO}_4$, and $\text{LiFe}_{0.96}\text{Pd}_{0.04}\text{PO}_4$ were synthesized using the sol-gel technique. XRD analysis indicates that the Li_3PO_4 impurity phase was detected for the Pd-doped samples, especially the $\text{LiFe}_{0.96}\text{Pd}_{0.04}\text{PO}_4$ sample, and that the lattice parameters of the Pd-doped samples decrease linearly as the amount of Pd^{2+} doping increases. Also, the particles become larger and they agglomerate following palladium incorporation, as shown in the SEM results. The electrochemical results show that the specific capacity of the LiFePO_4/C sample decreases with an increase in palladium content. The $\text{LiFe}_{0.96}\text{Pd}_{0.04}\text{PO}_4/\text{C}$ sample show an unsuitable electrochemical performance and poor rate cycling between samples, which could be attributed to its shrinking lattice parameters, large particle size, and the Li_3PO_4 impurity phase. As a result, palladium doping using the sol-gel method has an impact in the chemical composition, structure and electrochemical behavior of the LiFePO_4/C cathode material.

REFERENCES

- [1] A.K. Padhi, K.S. Nanjundaswamy, J.B. Goodenough, *Journal of The Electrochemical Society*, 144, 1188 (1997).
- [2] A. Yamada, S.C. Chung, K. Hinokuma, *Journal of The Electrochemical Society*, 148, A224 (2001).
- [3] Z.-R. Chang, H.-J. Lv, H.-W. Tang, H.-J. Li, X.-Z. Yuan, H. Wang, *Electrochimica Acta*, 54, 4595 (2009).
- [4] S. Franger, F. Le Cras, C. Bourbon, H. Rouault, *Electrochemical and Solid-State Letters*, 5, A231 (2002).
- [5] Y.-N. Xu, S.-Y. Chung, J.T. Bloking, Y.-M. Chiang, W.Y. Ching, *Electrochemical and Solid-State Letters*, 7, A131 (2004).
- [6] A. Kuwahara, S. Suzuki, M. Miyayama, *Journal of Electroceramics*, 24, 69 (2010).
- [7] D.-H. Kim, J. Kim, *Electrochemical and Solid-State Letters*, 9, A439 (2006).
- [8] N. Ravet, Y. Chouinard, J.F. Magnan, S. Besner, M. Gauthier, M. Armand, *Journal of Power Sources*, 97, 503 (2001).
- [9] X. Zhou, F. Wang, Y. Zhu, Z. Liu, *Journal of Materials Chemistry*, 21, 3353 (2011).
- [10] C.M. Doherty, R.A. Caruso, C.J. Drummond, *Energy & Environmental Science*, 3, 813 (2010).
- [11] Z.-R. Chang, H.-J. Lv, H. Tang, X.-Z. Yuan, H. Wang, *Journal of Alloys and Compounds*, 501, 14 (2010).
- [12] M. Wagemaker, B.L. Ellis, D. Lützenkirchen-Hecht, F.M. Mulder, L.F. Nazar, *Chemistry of Materials*, 20, 6313 (2008).
- [13] W.L. Liu, J.P. Tu, Y.Q. Qiao, J.P. Zhou, S.J. Shi, X.L. Wang, C.D. Gu, *Journal of Power Sources*, 196, 7728 (2011).
- [14] J. Ma, B. Li, H. Du, C. Xu, F. Kang, *Journal of Solid State Electrochemistry*, 16, 1 (2012).
- [15] D. Arumugam, G. Paruthimal Kalaigan, P. Manisankar, *Journal of Solid State Electrochemistry*, 13, 301 (2009).
- [16] X. Ou, G. Liang, L. Wang, S. Xu, X. Zhao, *Journal of Power Sources*, 184, 543 (2008).
- [17] M.-R. Yang, W.-H. Ke, *Journal of The Electrochemical Society*, 155, A729 (2008).
- [18] G.X. Wang, S. Bewlay, S.A. Needham, H.K. Liu, R.S. Liu, V.A. Drozd, J.-F. Lee, J.M. Chen, *Journal of The Electrochemical Society*, 153, A25 (2006).
- [19] H. Liu, C. Li, Q. Cao, Y.P. Wu, R. Holze, *Journal of Solid State Electrochemistry*, 12, 1017 (2008).
- [20] W.-J. Zhang, *Journal of The Electrochemical Society*, 157, A1040 (2010).
- [21] D. Morgan, A. Van der Ven, G. Ceder, *Electrochemical and Solid-State Letters*, 7, A30 (2004).
- [22] C. Ouyang, S. Shi, Z. Wang, X. Huang, L. Chen, *Physical Review B*, 69, 104303 (2004).
- [23] M.S. Islam, D.J. Driscoll, C.A.J. Fisher, P.R. Slater, *Chemistry of Materials*, 17, 5085 (2005).
- [24] S. Shi, L. Liu, C. Ouyang, D.-s. Wang, Z. Wang, L. Chen, X. Huang, *Physical Review B*, 68, 195108 (2003).
- [25] C.Y. Ouyang, S.Q. Shi, Z.X. Wang, H. Li, X.J. Huang, L.Q. Chen, *Journal of Physics: Condensed Matter*, 16, 2265 (2004).
- [26] D. Li, Y. Huang, D. Jia, Z. Guo, S.-J. Bao, *Journal of Solid State Electrochemistry*, 14, 889 (2010).
- [27] Z.-H. Wang, L.-X. Yuan, J. Ma, L. Qie, L.-L. Zhang, Y.-H. Huang, *Electrochimica Acta*, 62, 416 (2012).
- [28] J.B. Heo, S.B. Lee, S.H. Cho, J. Kim, S.H. Park, Y.S. Lee, *Materials Letters*, 63, 581 (2009).
- [29] J. Hong, X.-L. Wang, Q. Wang, F. Omenya, N.A. Chernova, M.S. Whittingham, J. Graetz, *The Journal of Physical Chemistry C*, 116, 20787 (2012).
- [30] Z.-H. Wang, Q.-Q. Pang, K.-J. Deng, L.-X. Yuan, F. Huang, Y.-L. Peng, Y.-H. Huang, *Electrochimica Acta*, 78, 576 (2012).
- [31] R.-r. Zhao, I.M. Hung, Y.-T. Li, H.-y. Chen, C.-P. Lin, *Journal of Alloys and Compounds*, 513, 282 (2012).
- [32] Y. Wang, Y. Yang, X. Hu, Y. Yang, H. Shao, *Journal of Alloys and Compounds*, 481, 590 (2009).

- [33]H. Gao, L. Jiao, W. Peng, G. Liu, J. Yang, Q. Zhao, Z. Qi, Y. Si, Y. Wang, H. Yuan, *Electrochimica Acta*, 56, 9961 (2011).
- [34]F. Lu, Y. Zhou, J. Liu, Y. Pan, *Electrochimica Acta*, 56, 8833 (2011).
- [35]C.S. Sun, Y. Zhang, X.J. Zhang, Z. Zhou, *Journal of Power Sources*, 195, 3680 (2010).
- [36]H. Liu, Q. Cao, L.J. Fu, C. Li, Y.P. Wu, H.Q. Wu, *Electrochemistry Communications*, 8, 1553 (2006).
- [37]H.C. Shin, S.B. Park, H. Jang, K.Y. Chung, W.I. Cho, C.S. Kim, B.W. Cho, *Electrochimica Acta*, 53, 7946 (2008).
- [38]S.-h. Wu, M.-S. Chen, C.-J. Chien, Y.-P. Fu, *Journal of Power Sources*, 189, 440 (2009).
- [39]P. Axmann, C. Stinner, M. Wohlfahrt-Mehrens, A. Mauger, F. Gendron, C.M. Julien, *Chemistry of Materials*, 21, 1636 (2009).
- [40]D.Y.W. Yu, K. Donoue, T. Kadohata, T. Murata, S. Matsuta, S. Fujitani, *Journal of The Electrochemical Society*, 155, A526 (2008).
- [41]C.S. Sun, Z. Zhou, Z.G. Xu, D.G. Wang, J.P. Wei, X.K. Bian, J. Yan, *Journal of Power Sources*, 193, 841 (2009).
- [42]G.A. Shafeev, J.-M. Themlin, L. Bellard, W. Marine, A. Cros, *Journal of Vacuum Science & Technology A: Vacuum, Surfaces, and Films*, 14, 319 (1996).
- [43]D. Shanmukaraj, G.X. Wang, R. Murugan, H.K. Liu, *Materials Science and Engineering: B*, 149, 93 (2008).